Ecotoxicology and Environmental Safety 123 (2016) 72–80

Contents lists available at ScienceDirect

Ecotoxicology and Environmental Safety

journal homepage: www.elsevier.com/locate/ecoenv

Detection of malformations in sea urchin plutei exposed to mercuric chloride using different fluorescent techniques

Isabella Buttino [a,*], Jiang-Shiou Hwang [b], Giovanna Romano [c], Chi-Kuang Sun [d], Tzu-Ming Liu [d], David Pellegrini [a], Andrea Gaion [a], Davide Sartori [a,e]

[a] Istituto Superiore per la Protezione e la Ricerca Ambientale, ISPRA_ STS-Livorno, Piazzale dei marmi 12, 57123, Italy
[b] Institute of Marine Biology, National Taiwan Ocean University, Keelung 20224, Taiwan
[c] Stazione Zoologica Anton Dohrn, Villa Comunale, 80121 Napoli, Italy
[d] Graduate Institute of Photonics and Optoelectronics and Department of Electrical Engineering, National Taiwan University, Taipei 10617, Taiwan
[e] CAISIAL, Academic Centre for Innovation and Development in the Food Industry, 80055 Portici (Na), Italy

ARTICLE INFO

Article history:
Received 25 March 2015
Received in revised form
22 July 2015
Accepted 23 July 2015
Available online 5 August 2015

Keywords:
Harmonic generation microscopy
Two-photon microscopy
Confocal microscopy
Skeletal rod
Apoptosis

ABSTRACT

Embryos of Mediterranean sea urchin *Paracentrotus lividus* and subtropical *Echinometra mathaei* were exposed to 5,10, 15 and 20 μg L^{-1} and to 1, 2, 3 and 4 μg L^{-1} mercuric chloride ($HgCl_2$), respectively. The effective concentration (EC_{50}) inducing malformation in 50% of 4-arm pluteus stage (P4) was 16.14 μg L^{-1} for *P. lividus* and 2.41 μg L^{-1} for *E. mathaei*. Two-photon (TP), second (SHG) and third harmonic generation (THG) microscopy techniques, TUNEL staining, propidium iodide (PI) and Hoechst 33342 probes were used to detect light signals or to stain apoptotic and necrotic cells in fixed and alive plutei. Signals were detected differently in the two species: TP fluorescence, commonly associated with apoptotic cells, did not increase with increasing $HgCl_2$ concentrations in *P. lividus* and in fact, the TUNEL did not reveal induction of apoptosis. PI fluorescence increased in *P. lividus* in a dose-dependent manner, suggesting a loss of cell permeability. In *E. mathaei* plutei TP fluorescence increased at increasing $HgCl_2$ concentrations. THG microscopy revealed skeletal rods in both species. Different fluorescent techniques, used in this study, are proposed as early-warning systems to visualize malformations and physiological responses in sea urchin plutei.

1. Introduction

Mercury (Hg) is one of the most toxic and persistent elements in the environment, deriving both from natural and anthropogenic sources. This metal can enter the ecosystem through the breakdown of minerals, although significant amounts originate as a result of human activities and discharges from metal smelting, coal-burning power plants, municipal waste incineration, coal and other fossil fuel combustion (Satoh, 2000). In aquatic ecosystems, mercury is present mainly in inorganic elemental (Hg°, Hg^{2+}) or organic methylated form and its bioavailability is influenced by physical-chemical factors such as pH, dissolved organic carbon or temperature of the water (Driscoll et al., 1994). Between the two ionized states, the bivalent form is more stable and more frequently found, and can bond with chloride ($HgCl_2$) in salt water. Mercury concentrations in aquatic environments are highly variable, ranging from very low concentrations in open ocean to concentrations as high as 16 μg L^{-1} in very polluted areas close to industrial discharges (Plaschke et al., 1997; De Riso et al., 2000).

Toxic effects of mercury have been widely studied on fish (Driscoll et al., 1994; Devil, 2006; Sinaie et al., 2010), due to their relevance in human consumption. On the other hand, the impact of mercury on marine environment has been investigated using animal models, belonging to different trophic levels, and taking into consideration various end-points such as behavior, reproduction, embryo and larval mortality or morbidity (Fernandez and Beiras, 2001). In ecotoxicology studies, echinoderms are considered excellent bioindicators due to their dual role in pelagic and benthic compartments (Bellas et al., 2005; Salamanca et al., 2009). Furthermore, echinoderm gametes are easy to collect and fertilization and larval development are well known (Pagano et al., 1986). Studies on the toxicity of mercury on sea urchin species have mainly been focused on the evaluation of the effective concentration (EC_{50}) inducing 50% embryo and larval mortality, as well as deformities, or sperm fertilization inhibition (Fernandez and Beiras, 2001; Warnau et al., 1996).

In this study we analyzed the effect of increasing

* Corresponding author.
E-mail address: isabella.buttino@isprambiente.it (I. Buttino).

http://dx.doi.org/10.1016/j.ecoenv.2015.07.027
0147-6513/

concentrations of mercuric chloride ($HgCl_2$) on the larval development of two different sea urchin species: *Echinometra mathaei*, the most ubiquitous and abundant shallow-water sea urchin in tropical and subtropical regions, and *Paracentrotus lividus. E. mathaei* is commonly found at depth up to 130 mt and in a temperature range between 24 and 27 °C. It has a flexible behavior and diet, high reproduction and recruitment rates and low resource requirements (McClanahan and Muthiga, 2007). Although genetic, morphological, biochemical, ecological and reproductive studies have been carried out on *Echinometra* species, few data are available on its sensitivity to organic and inorganic contaminants (Kominami and Takata, 2003; Mahdavi et al., 2008; Sadripour et al., 2013). *Paracentrotus lividus* is common in the temperate Mediterranean areas, with winter water temperatures of around 11 to 12 °C and summer temperatures ranging from 18 to 25 °C (Boudouresque and Verlaque, 2007). This species has largely been used as a model animal to study the impact of toxicants (Bellas et al., 2008; Pinsino et al., 2010; Gaion et al., 2013) or natural toxins (Romano et al., 2011, 2003, 2010).

Here we evaluated the effective concentration of $HgCl_2$ inducing malformations in the 4-arm plutei stage (P4) in both temperate and subtropical species. Furthermore, harmonic generation (HGM) and two-photon (TP) microscopy techniques were used to verify whether fluorescence signals could be associated with chemical stress. Harmonic generation and TP microscope are the least invasive laser scanning techniques enabling visualization of autofluorescent and endogenous harmonic generation signals from the whole-mount samples, with submicron spatial resolution and without the use of fluorescent probes. Optical sections along the depth of the sample can detect different cell morphology and physiological activity (Chu et al., 2003). Furthermore, we used TUNEL staining to detect apoptotic cells in *P. lividus* P4 stage exposed to $HgCl_2$, propidium iodide (PI) to visualize necrotic cells in live plutei and Hoechst 33342 to stain cell nuclei. Apoptosis or programmed cell death is a form of cell suicide showing characteristic morphological and biochemical alterations such as cell shrinkage, blebbing and activation of specific caspases that lead to enzymatic breakdown of DNA (Lockshin et al., 1998). Apoptosis is a physiological process occurring during embryo development and metamorphosis (Roccheri et al., 2002; Thurber and Epel, 2007; Agnello and Roccheri, 2010), but can also be activated by external stimuli such as the presence of bioactive molecules and pollutants (Romano et al., 2003; Agnello et al., 2007). Different fluorescent techniques applied in this study, could be used as early stress indicators in sea urchin bioassay tests.

2. Materials and methods

2.1. Gamete collection

P. lividus and *E. mathaei* adults were collected from an intertidal rocky site along the coast of Livorno (Italy) [43° 25′ 31.79″ N, 10° 23′ 37.51″ E] and Keelung (Taiwan) [25° 8′ 30.79″ N, 121° 48′ 11.79″ E] respectively, and immediately transported in an insulated box to the laboratory. Animals were injected with 1 ml of 0.5 M KCl solution into the coelom, through the peristome, to obtain gametes, soon after their arrival. Sperm obtained from at least three males was collected dry from each male using a Pasteur pipette, pooled and conserved in an Eppendorf tube at 4 °C until fertilization within 2 h. Sperm concentration was determined diluting 50 µl of semen in 25 ml tap water to enlarge sperm head, through osmotic shock, which was then measured with a hemocytometer (Thoma chamber) under the Olympus inverted-microscope (Milan, Italy) using a 40*x* objective. Oocytes obtained from at least three females were pooled into 1 L beaker filled with 0.22 µm filtered seawater (FSW) collected at the corresponding sampling site (36 ± 1 psu salinity, $pH = 8.0 \pm 0.2$). The final concentration of 1000 eggs mL^{-1} was prepared by counting subsamples of a known volume with the inverted Olympus microscope at 4*x* objective. Fertilization occurred diluting sperm and eggs in 1 L FSW beaker at 15,000:1 and 10,000:1 sperm:egg ratio, for *P. lividus* and *E. mathaei*, respectively (Rahman et al., 2000; Lera and Pellegrini, 2006). Few minutes after fertilization, an aliquot of embryos was observed under the inverted microscope to verify the presence of the fertilization membrane. The acceptability of the sample was fixed at a fertilization rate above 90%, as also suggested by other authors (from 70% to 95%) (Warnau et al., 1996; Arizzi Novelli et al., 2002; Lera and Pellegrini, 2006).

2.2. Incubation experiments

Each solution was prepared dissolving 135.75 g of $HgCl_2$ in 500 mL bi-distilled water (BDW) to obtain a final concentration of 1M $HgCl_2$ solution. Nominal concentrations of 10, 20, 30, 40, 50, 80, 100, 150, 200 and 250 µg L^{-1} $HgCl_2$ (corresponding approximatively to 3.6–92 µM $HgCl_2$) were then obtained diluting 1M solution in FSW and stirring at the test temperature (1 µg L^{-1} $HgCl_2$ corresponds to 0.74 µg L^{-1} Hg^{2+}). One milliliter of each solution was then added to 9 ml FSW in each well plate containing about 1000 *P. lividus* and *E. mathei* embryos, to obtain final concentrations of 5, 10, 15, 20 and 25 µg L^{-1} for *P. lividus* and 1, 2, 3, 4 and 8 µg L^{-1} for *E. mathaei. Paracentrotus lividus* embryos were maintained at 18 ± 2 °C (Cakal Arslan et al., 2007) while *E. mathaei* where maintained at 24 ± 1 °C (Kominami and Takata, 2003). An untreated control for each species was incubated in FSW alone; six replicates for each condition were applied.

Larval growth followed until the controls reached P4 stage for more than 80%. For *P. lividus* this stage occurred 72 h after fertilization, 48 h for *E. mathaei*. The acceptability of the results was fixed when the percentage of normal plutei was higher than 80% in the controls. Normal and abnormal P4 were identified according to Pagano et al. (1986); the fully developed P4 larvae were considered normal, whereas retarded gastrulae, preastrulae, prism stages and those malformed (showing defects in the skeleton and/or digestive apparatus) were considered abnormal (De Nicola et al., 2007). Median effective concentration inducing 50% of abnormal P4 stages (EC_{50}) was determined for each species, considering the percentage of abnormal P4 stage in each concentration.

2.3. Harmonic generation microscopy analyses

To verify HGM or TP fluorescent signals in living plutei, P4 embyos from both sea urchin species were observed with the second (SHG) and third harmonic generation (THG) microscopy techniques and TP contrast using an adapted upright microscope Olympus BX51 microscope (Taipei, Taiwan) (Hsieh et al., 2008). The scanned SHG and THG images were obtained with a 60x water immersion objectives at numerical aperture of 1.2. The HGM microscopy system is based on a femto-second Cr:forsterite laser operating at wavelengths (λ) of 1230 nm, which can achieve deepest penetration and causes less damage compared with the most commonly used Ti:sapphire laser (700–1000 nm λ) (Chen et al., 2001; Sun et al., 2004). Harmonic generation microscopy is related to the interaction of intense light with matter; in particular the SHG intensity generated depends on the square of the incident light intensity (Chu et al., 2002) and signals are generated at dense, non-centro symmetric structures, such as collagen fibers and striated muscle myosin (Rehberg et al., 2011). The THG fluorescence generated depends on the cubic of the incident light intensity and associated signals were found to be associated with

optical property in homogeneity in unfixed tissues. Furthermore, it can illustrate cell boundaries or the vesicles distribution (Hsieh et al., 2008). By using such intrinsic contrasts, fluorescent probes are not required and dye-related problems (permeability, photodamage, phototoxicity, photobleaching, availability or eventual toxicity) can all be eliminated. Analyses were performed 3 times with 3 replicates and at least 10 embryos, among the most abundant larval stage present in each treatment, were observed.

2.4. TUNEL staining

P. lividus embryos exposed to 5, 10, and 15 μg L^{-1} $HgCl_2$ were stained with terminal deoxy-nucleotidyl-transferase-mediated dUTP nick end labelling (TUNEL, Promega Italia, Milan, Italy). This assay is able to detect apoptotic cells in fixed samples, which appeared with positive, green fluorescent nuclei (Gavrieli et al., 1992). When untreated controls reached the P4 stage a group of almost 200 embryos was fixed for 1 h in 4% paraformaldehyde (PFA), rinsed in phosphate buffer saline solution (PBS) and incubated at 4 °C in 0.1% triton in PBS for 30 min. After being rinsed twice in PBS and once in PBS with 1% bovine serum albumin (SIGMA ALDRICH, Milan, Italy), plutei were incubated for 1 h at 37 °C in the TUNEL, according to the manufacturer instructions. The enzyme was diluted 1:10 with the equilibration buffer to avoid unspecific background. An additional aliquot of the same plutei (almost 50 larvae) was pre-treated for 10 min with 1 Unit mL^{-1} DNAase (Biolab, UK) at 37 °C before TUNEL staining. Another group of almost 50 larvae was incubated with TUNEL labeling without the enzyme, as a negative TUNEL control. All samples were then observed with an inverted ZEISS 510 confocal laser scanning microscopy (CLSM, Oberkochen, Germany) using a 488 nm λ laser.

2.5. Hoechst and propidium iodide staining

Propidium iodide and Hoechst 33342 (Sigma-Aldrich, Milan) are viable probes used to stain not-fixed samples; PI marks dead cells with compromised cell-membrane integrity in red, while Hoechst 33342 stains the nuclei of both living and dead cells specifically in blue (Fried et al., 1976). An aliquot of almost 200 alive *P. lividus* plutei exposed to 5, 10, and 15 μg L^{-1} $HgCl_2$ were incubated 30 min in 1 μg mL^{-1} Hoechst 33342 and 15 min in 2 μg mL^{-1} PI. After being rinsed in FSW samples were fixed for 1 h in 4% PFA at room temperature, then rinsed again in PBS and observed with the inverted CLSM using 405 and 543 nm λ lasers for Hoechst 33342 and PI, respectively.

2.6. Statistical analyses

Probit analysis was used to estimate the concentration that caused an abnormal development in 50% (EC_{50}) of P4 stage (Hamilton et al., 1978). To guarantee the accuracy of the test, EC_{50} and coefficient of variation were calculated. Analyses of variance (One-way ANOVA) and Student–Newman–Keuls (SNK) tests were applied to evaluate differences in deformed P4 embryos between treatments. The SNK method was used as post-hoc test, whenever a significant difference between tested concentration was revealed by ANOVA.

3. Results

The percentage of normally developed *P. lividus* and *E. mathei* plutei exposed to different $HgCl_2$ concentrations is reported in Fig. 1. A significant decrease in the percentage of normal *P. lividus* P4 stages was observed at concentrations ≥ 15 μg L^{-1} $HgCl_2$ (73.8 ± 7.5% standard deviation s.d., SNK test $p < 0.05$). At 20 μg L^{-1} $HgCl_2$ only 6 ± 2.1% were normally developed plutei. The subtropical species *E. mathaei* exhibit the highest sensitivity in respect to the Mediterranean sea urchin; in fact, at 2 μg L^{-1} $HgCl_2$ the percentage of normal P4 was significantly reduced (51 ± 3.6%, SNK test $p < 0.01$) and at 3 μg L^{-1} $HgCl_2$ this percentage was further reduced to less than 40 ± 6.7%. Normal plutei sharply declined to 18.3 ± 4.4% at 4 μg L^{-1} $HgCl_2$ and to less than 10% at 8 μg L^{-1}. The EC_{50} calculated for *E. mathei* was 2.41 ± 1.7 μg L^{-1} whereas for *P. lividus* this was 16.14 ± 1.5 μg L^{-1} $HgCl_2$. Living P4 stages exposed to $HgCl_2$ were observed with TP, SHG and THG microscopy to verify whether autofluorescent and HG signals were differently detected in plutei exposed at increasing concentrations (Fig. 2). *P. lividus* plutei showed very weak TP (Fig. 2a–e) and SHG signals in all treatments (Fig. 2f–l). Few spots of TP fluorescent signals were visible in plutei exposed from 5 to 15 μg L^{-1} $HgCl_2$ (Fig. 2b–d), whereas an unspecific background was observed in plutei exposed to the concentration of 20 μg L^{-1} $HgCl_2$ (Fig. 2e). Samples exposed to concentrations from 5 to 15 μg L^{-1} $HgCl_2$ showed SHG signals in the same fluorescent cells observed with TP (Fig. g–i) and no specific fluorescence was observed at the highest concentration (Fig. 2l). Signals from THG revealed a strong contrast of skeletal rods in the controls (Fig. 2m) that disappeared in almost all the exposed plutei (Fig. 2n, o, q). At 15 μg L^{-1} $HgCl_2$ few spicules appeared THG-bright in only one arm (Fig. 2p). *Paracentrotus lividus* plutei stained with the TUNEL are shown in Fig. 3. Control plutei observed in transmitted light appeared normally developed and negatively stained with the TUNEL (Fig. 3a, b) suggesting that at this stage physiological induction of apoptosis was not activated. In the positive DNAase-treated sample, DNA breaks are similar to those induced by apoptosis and nuclei were fluorescent in green (Fig. 3c is a merge of bright light and fluorescent microscopy images). Fig. 3d shows an untreated control pluteus stained with PI (red) and Hoechst 33342 (violet); due to DNA staining only the violet fluorescence was evident, whereas red fluorescence (dead cells) was not visible. An increasing red fluorescence was observed in plutei exposed at the increasing $HgCl_2$ concentrations suggesting that cell membrane permeability was progressively lost in these plutei with a dose-dependent correlation (Fig. 3f, h, l). Green fluorescence due to the TUNEL was evident only in a few cells in plutei exposed from 5 to 15 μg L^{-1} $HgCl_2$ (Fig. 3e, g, l, arrows), similar to those observed with TP microscopy at the same concentrations (Fig. 2b, c, d).

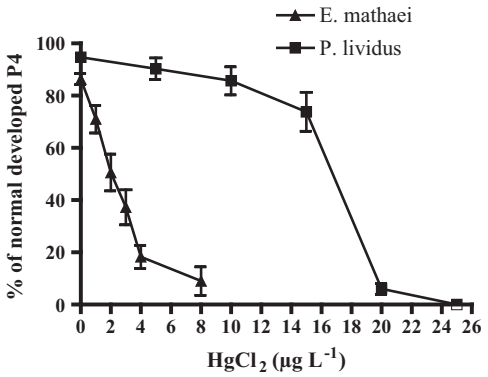

Fig. 1. Percentage of normally developed 4-arm larval stage of *Paracentrotus lividus* and *Echinometra mathaei* incubated soon after fertilization at different $HgCl_2$ concentrations. Each data point represents the mean of three independent experiments, while the vertical bars represent standard deviation.

Two-photon, SHG and THG microscopy images of *E. mathaeii* plutei are shown in Fig. 4. Plutei exposed to 2 and 4 μg L^{-1} $HgCl_2$ observed with TP microscopy showed a significant increase in fluorescent signals (Fig. 4c, d), with respect to the control group (Fig. 4a), while, more than 80% of malformed plutei at 4 μg L^{-1}

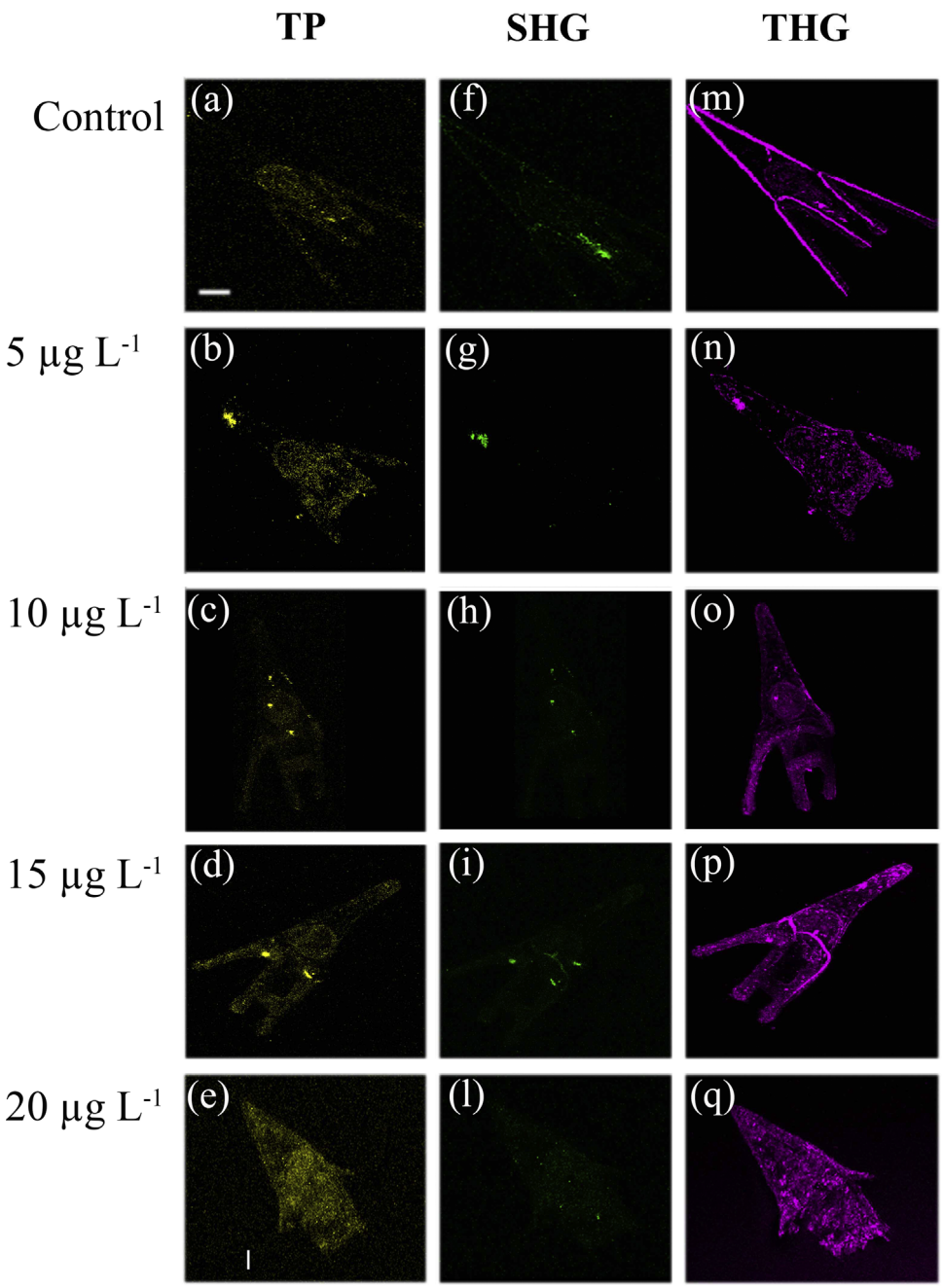

Fig. 2. *Paracentrotus lividus* plutei exposed to different $HgCl_2$ concentrations (row) have been observed with different fluorescent techniques (column). (a–e) two photon microscopy (TP); (f–l) second harmonic generation microscopy (SHG); (m–q) third harmonic generation microscopy (THG). (Bar = 40 µm).

$HgCl_2$ lost the signal (Fig. 4e). SHG signals were low in all the observed plutei at any concentration (Fig. 4f–i), whereas THG fluorescence marked spicules in all treated samples, including strongly deformed plutei (Fig. 4m–q).

4. Discussion

Embryos of two sea urchin species, one inhabiting temperate areas and the second subtropical sea, were exposed to different $HgCl_2$ concentrations; EC_{50} was determined taking into consideration the percentage of abnormal P4 stage. This stage was deemed the end-point, allowing us to detect malformations induced by mercury in both species. Malformations in the P4 stage were analyzed in terms of defects to shape and skeletal rods, using the following optical techniques: i) HGM and TPF microscopy, which facilitates analysis of living, whole-mount plutei without the use of fluorescent probes; ii) the classical TUNEL staining protocol, which identify early apoptosis induction in fixed samples, and iii) the vital fluorescent probes PI and Hoechst 33342, chemicals that penetrate only dead, necrotic cells with compromised cell membrane integrity, or stains nucleic acids respectively.

In terms of dose–response effects, results showed an increasing number of malformed P4 stage at higher Hg concentrations. However, the two species showed different sensitivity; the most sensitive species was the subtropical *E. mathaei*, with an EC_{50} value that was 8-folds lower compared to the temperate sea urchin *P. lividus*. Toxicity of $HgNO_3$ on *E. mathaei* species was studied by Sadripour et al. (2013) which found variable and higher EC50 values (17/42 µg L^{-1} $HgNO_3$), compared to our results. However, the

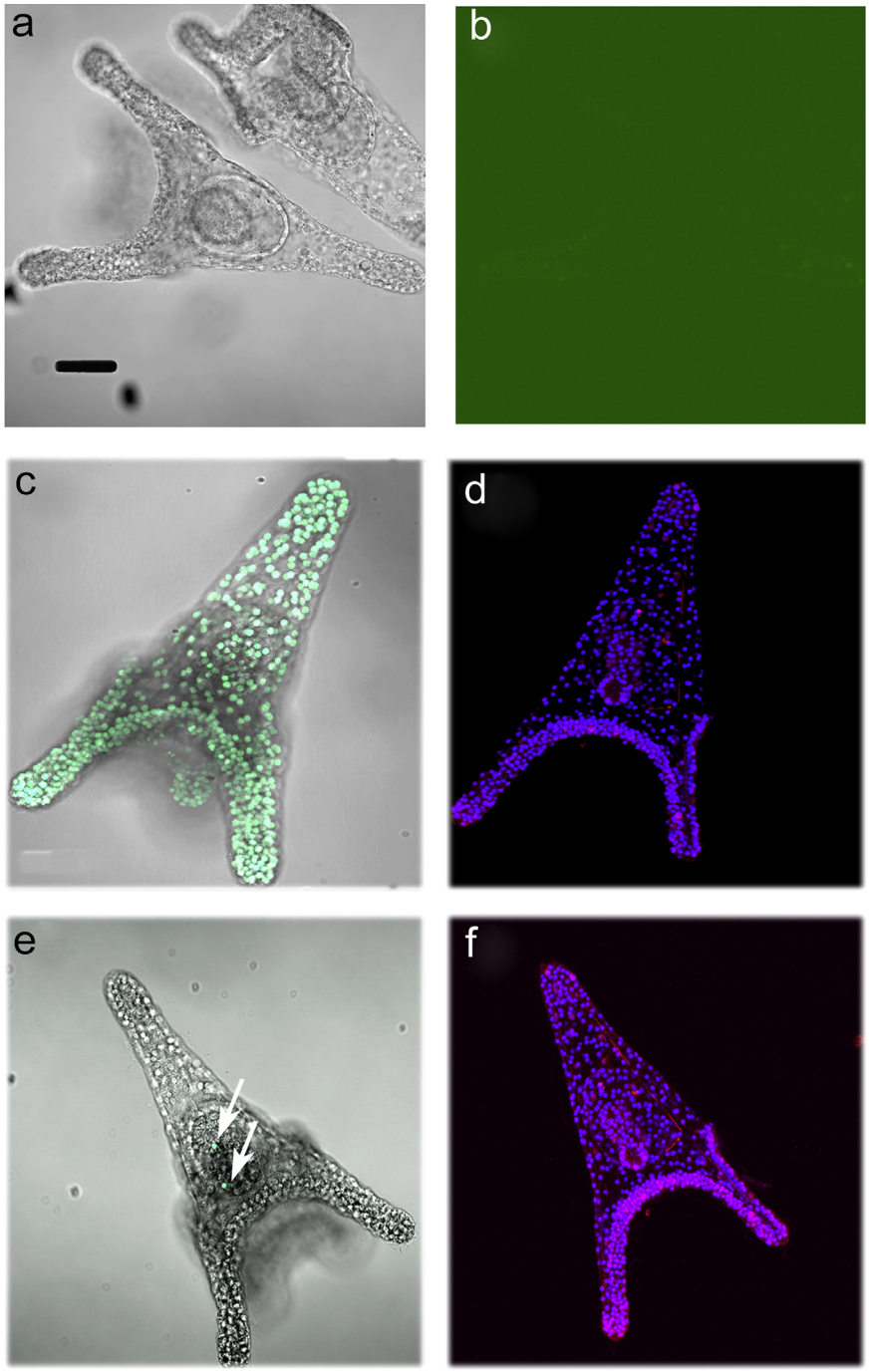

Fig. 3. *Paracentrotus lividus* plutei observed with confocal laser scanning microscopy. (a), (b), (c), (e) and (g) fixed plutei stained with the TUNEL to detect apoptosis, observed in transmitted light and in fluorescence using a 488 nm wavelength laser to detect apoptotic cells. (d), (f), (h), (l) living plutei stained with propidium iodide (PI) and observed with a 543 nm wavelength laser (red), to detect necrotic cells, and with Hoechst 33342, observed with a 405 nm wavelength laser (violet), to detect nucleic acids. (a) Untreated control plutei observed in transmitted light and (b) the corresponding TUNEL staining pluteus did not show any fluorescence even at a very high contrast (green background). (c) Pluteus treated with DNAse enzyme, in which TUNEL stains fluorescent nuclei in green (positive control). The figure is a merge of the transmitted light microscopy and the fluorescent images. (d) Untreated, control pluteus stained with the Hoechst 33342 probe and the PI showing only the violet fluorescence of nucleic acids. (e) Pluteus developed within 5 $\mu g\ L^{-1}$ $HgCl_2$ showing two cells positively stained with TUNEL (arrows). (f) Pluteus exposed as in (e) showing an increase in red fluorescence. (g) Pluteus developed within 10 $\mu g\ L^{-1}$ $HgCl_2$ appeared with two cells positively stained with TUNEL (arrows). (h) Pluteus exposed as in (g) showing deformities and a strong red fluorescence in the whole body. (i) Pluteus developed within 15 $\mu g\ L^{-1}$ $HgCl_2$ appeared severely deformed with few nuclei positively stained in green (arrows). (l) Plutei exposed as in (i) strongly malformed and highly fluorescent in red. (Bar = 40 μm).

authors incubated embryos after the first embryonic cleavage while, in our study, embryos were incuabated immediately after fertilization. It is well known that heavy metal toxicity is associated with the incubation stage of sea urchins, with gametes and zygotes being more sensitive than later developmental stages (Kobayashi, 1995; Kobayashi and Okamura, 2004).

For *P. lividus*, results are comparable with those reported by Kobayashi (1995) in which deformed plutei were recorded at Hg concentrations above to 6.8 $\mu g\ L^{-1}$. The concentration of total mercury in aquatic environment is highly variable, with values ranging from less than 3 $ng\ L^{-1}$ in unpolluted seawater to more than 10 $\mu g\ L^{-1}$ in polluted coastal and estuarine areas (De Riso

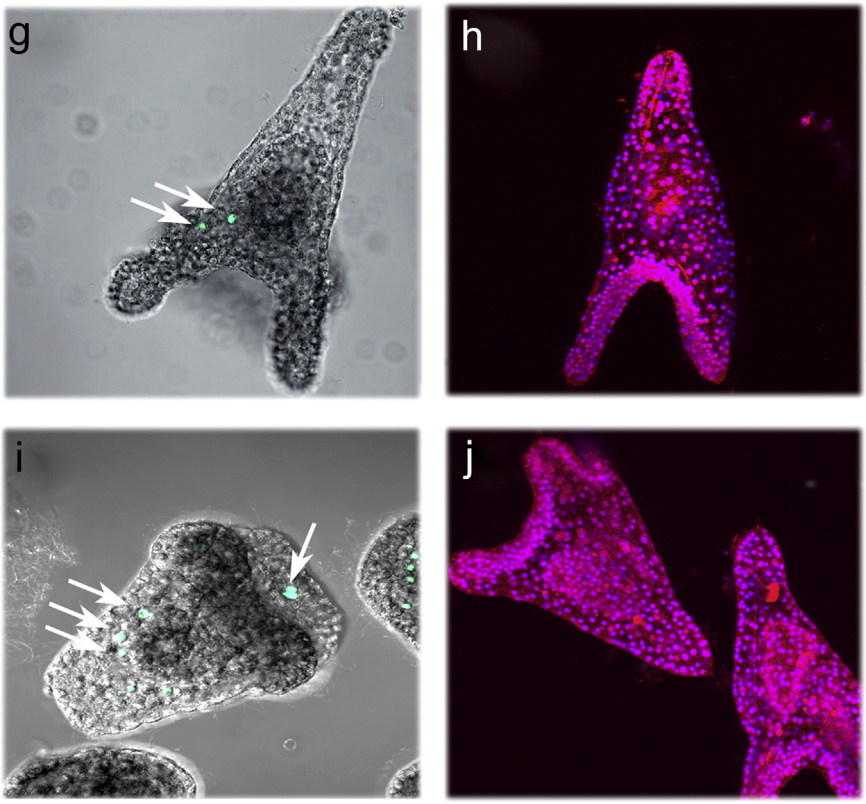

Fig. 3. (*continued*)

et al., 2000), where sea urchin development could be disrupted.

It has been reported that mercury toxicity increases with higher temperatures for a wide range of species (Chaudhary and Gupta, 2006; Tsui and Wang, 2006; Fernández and Beiras, 2001). Our study does not rule out the possibility that the different temperatures used in our protocol could influence the different sensitivity recorded for the two species. However, larvae of *P. lividus* and *E. mathaei* were exposed to their typical environmental median temperatures, which can be considered as the actual exposure scenario during their life cycle. In addition, tropical organisms live in more stable environments, likely explaining the great sensitivity of *E. mathaei* compared with eurytherm Mediterranean species *P. lividus*.

The sea urchin embryo development test is considered a standard bioassay by which to evaluate the toxicity of specific pollutants (Gaion et al., 2013; Beiras et al., 2003). The ratio between normally and abnormally developed larvae (such as deformities in skeletal rods) is an important evaluation criterion and should be clearly determined and described. Recently, skeletal integrity has been suggested as a more sensitive criterion with respect to the classical normally-shaped larval description or EC_{50} determination. Carballeira et al. (2012) classified abnormalities according to the severity of skeletal alteration. In our study, we showed that THG microscopy was able to detect skeletal rod (see Figs. 2 and 4) and this technique can be useful to investigate skeletal malformations during pluteus development. Skeletal alterations in sea urchins have been observed after exposure to different classes of toxicants, including heavy metals and effluents, therefore their description can be considered a fast early-warning test in bioassay studies. In both *P. lividus* and *E. mathaei* malformations of P4, induced by $HgCl_2$, is dose-dependent, although THG microscopy revealed different mechanisms of toxicity in the two species: a loss of THG signal in the skeleton of *P. lividus* was observed with all tested concentrations could be due to incorrect tissutal organization in the skeletal structures (Fig. 2). By contrast, the THG signals by skeletal rod fluorescence was always evident in *E. mathaei*, suggesting correct tissue formation (Fig. 4). This also suggests that the induced morphological anomalies were not determined by incorrect skeletal structures. This technique is useful as a fast screening assay of the anomalies induced by toxicants during sea urchin larval development.

In the last decade, detection of apoptosis or programmed cell death in marine invertebrates exposed to bioactive molecules has opened new perspectives in marine ecotoxicology and physiology studies (Romano et al., 2003, 2010; Agnello et al., 2007; Ianora et al., 2004; Buttino et al., 2011). The feasibility of identifying apoptosis before the appearance of macroscopic aberrations is useful for predicting toxic effects (Buttino et al., 2011). Apoptosis in sea urchin occurs as physiological process to mold the organism during larval development (Roccheri et al., 2002; Voronina and Wessel, 2001), but it could also be activated in response to different external stresses (Romano et al., 2003). Recently, Filosto et al. (2008) demonstrated that Cd^{2+} induced an apoptotic response in *P. lividus* embryos exposed to subacute/sublethal concentrations. It was previously demonstrated that apoptosis can be activated to remove cells with a heavily damaged DNA structure: this process can be considered as a part of a defense strategy from pollutant-induced toxicity (Filosto et al., 2008). There is growing evidence that mercury is an effective apoptogenic toxicant for humans (Sutton and Tchounwou, 2006); to our knowledge, however, this aspect has never been investigated in marine organisms. In the present study, different approaches were applied to detect apoptosis in sea urchin plutei: the classical protocol using the TUNEL and HGM microscopy. It is interesting to note that *P. lividus* plutei exposed in 5–15 $\mu g\ L^{-1}$ $HgCl_2$ showed only few positive cells marked with the TUNEL and signals were similar to those found using TP and SHG microscopy (Figs. 2 and 3). Our results suggest that a general increase in TP signals, recorded in *E. mathei*

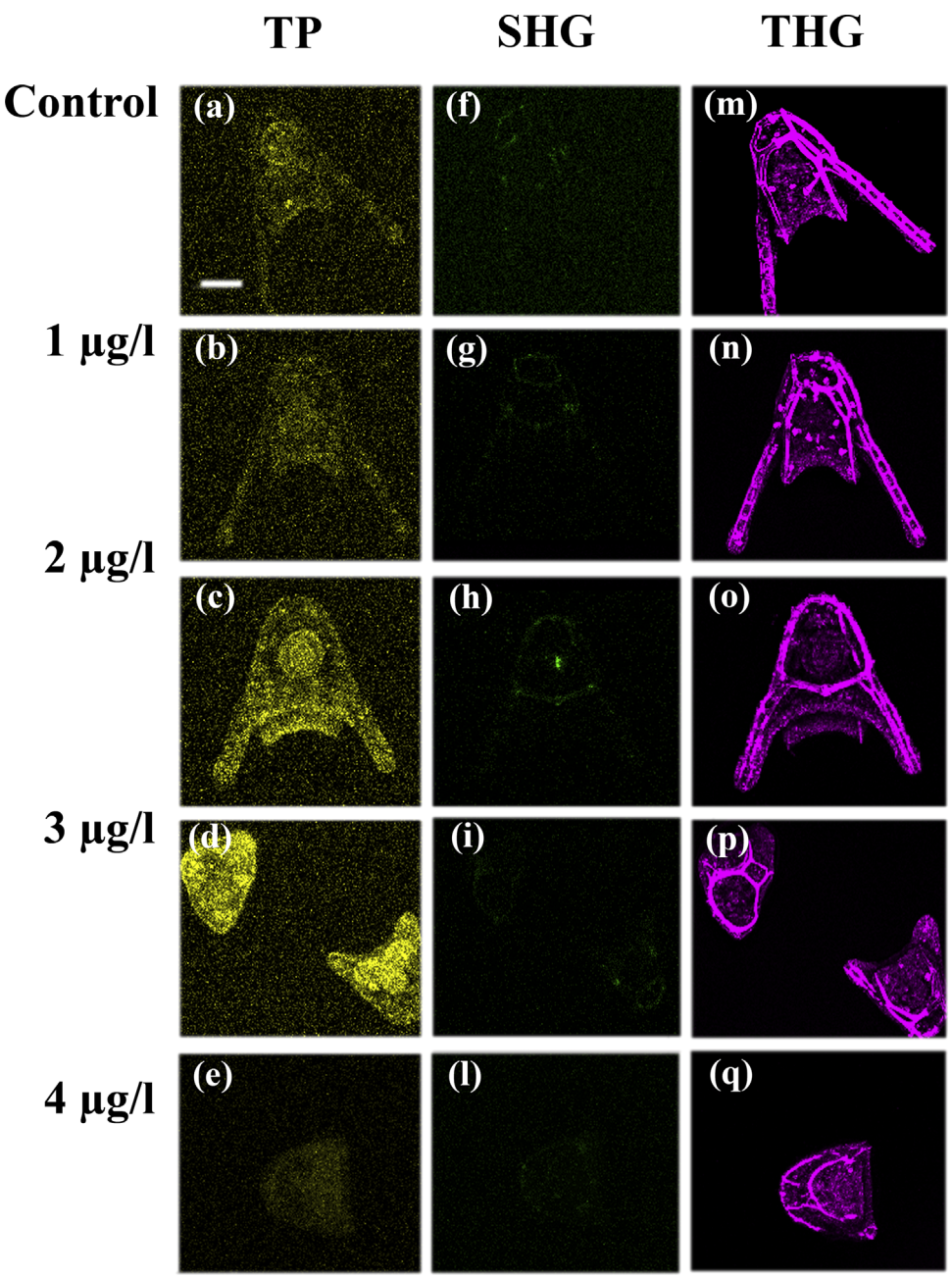

Fig. 4. *Echinometra mathaei* plutei exposed to different $HgCl_2$ concentrations (row) were observed using different fluorescent techniques (column). (a–e) two photon microscopy (TP); (f–l) second harmonic generation microscopy (SHG); (m–q) third harmonic generation microscopy (THG). (Bar = 64.3 μm).

plutei exposed to increasing $HgCl_2$ concentrations, could be due to an apoptotic-like mechanism. At the highest $HgCl_2$ concentration TP autofluorescence disappeared in both species, probably due to an unspecific inhibition of metabolic activities occurring in such highly abnormal plutei. Previous studies have confirmed that strong TP autofluorescence is associated with apoptotic cells; for example TP signals were associated with apoptotic bodies in the hind brain of zebrafish (Hsieh et al., 2008) and in copepods (Buttino et al., 2011).

In *P. lividus* an increase in red fluorescence associated with the PI probe was clearly observed starting from 5 $\mu g\, L^{-1}$ $HgCl_2$, suggesting that cell permeability increased in a dose-dependent manner as a consequence of chemical stress. This result is consistent with the hypothesis of an interaction between Hg^{2+} and cell transport/membrane permeability processes (Bonacker et al., 2004). Changes in membrane permeability due to physical or chemical stress is well known (Bischof et al., 1995), in particular, exposure to inorganic mercury altered calcium channel conductance in human cell lines with corresponding effects on membrane permeability (Bischof et al., 1995; Parran et al., 2001; Hajela and Peng, 2003). This phenomenon has never been observed in *P. lividus* embryos; $HgCl_2$ was able to increase membrane fluidity by stimulating interaction with Ca^{2+} channels (Allemand et al., 1988). In addition, Allemand et al. (1993) demonstrated that $HgCl_2$ can alter the intracellular pH of *P. lividus* fertilized sea urchin eggs, prompting an increase of Ca^{2+} influx corresponding an H^+ mobilizations in the acidic intracellular compartments. Alternatively, PI staining could be associated with the presence of organelles such as lysosomes, which concentrate heavy metals as a de-toxification mechanism (Viarengo, 1989). It is also known that PI-positive staining, in living cells, could be associated with high RNA contents, which may not necessarily be followed by protein

synthesis (Rieger et al., 2010). Further investigations are needed to better clarify cellular mechanism induced by $HgCl_2$ and it remains to be verified whether cell permeability increases, thus also exposing P4 larvae to other toxicants. At present, PI can be proposed as a rapid *in vivo* probe to detect chemical stress in *P. lividus* plutei exposed to mercury.

In conclusion, our results suggest that two sea urchin species activate different mechanisms in response to mercury exposure; the less-sensitive temperate species lost selective permeability of the membrane, and the apoptotic mechanism is not induced at the tested concentrations. In the more sensitive tropical species, plutei showed an increase in apoptotic-like signals. These different approaches can be useful for the rapid evaluation of toxicity in living organisms and can be considered early-warning systems in bioassay tests.

Acknowledgements

This research has been partially funded by the National Science Council of Taiwan, grant from the Summer Program 2011 and a bilateral project comprising the Stazione Zoologica Anton Dohrn, Naples, Italy and the National Science Council of Taiwan [Grant no. NSC 101-2923-B-019-001-MY2].

We are extremely grateful to all the staff of STS-ISPRA Livorno, the Institute of Marine Biology of National Taiwan Ocean University, the Molecular Imaging Center at National Taiwan University and the National Health Research Institute, for technical and qualified assistance during the project.

Appendix A. Supplementary material

Supplementary data associated with this article can be found in the online version at http://dx.doi.org/10.1016/j.ecoenv.2015.07.027.

References

Satoh, H., 2000. Occupational and environmental toxicology of mercury and its compounds. Indus. Health 38, 153–164.
Driscoll, C.T., Yan, C., Schofield, C.L., Munson, R., Holsapple, J., 1994. The mercury cycle and fish in the Adirondak Lakes. Environ. Sci. Technol. 28, 136–143.
Plaschke, R., Dal Pont, G., Butler, E.C.V., 1997. Mercury in waters of the Derwent Estuary - sample treatment and analysis. Mar. Pollut. Bull. 34, 177–185.
De Riso, R., Waeles, M., Mombet, P., Chaumery, C.J., 2000. Measurements of trace concentrations of mercury in sea water by stripping chronopotentiometry with gold disk electrode: influence of copper. Anal. Chim. Acta 410, 97–105.
Devil, E.W., 2006. Acute toxicity, uptake and histopathology of aqueous methyl mercury to fathead minnow embryos. Ecotoxicology 15, 97–110.
Sinaie, M., Bastami, K.D., Ghorbanpour, M., Najafzadeh, H., Shekari, M., Haghparast, S., 2010. Metallothionein biosynthesis as a detoxification mechanism in mercury exposure in fish, spotted scat (Scatophagus argus). Fish Physiol. Biochem. 36, 1235–1242.
Fernandez, N., Beiras, R., 2001. Combined toxicity of dissolved mercury with copper, lead and cadmium on embryogenesis and early larval growth of the *Paracentrotus lividus* sea-urchin. Ecotoxicology 10, 263–271.
Bellas, J., Granmo, A., Beiras, R., 2005. Embryotoxicity of the antifouling biocides zinc pyrithione to sea urchin (*Paracentrotus lividus*) and mussel (*Mytilus edulis*). Mar. Pollut. Bull. 50, 1382–1385.
Salamanca, M.J., Fernández, N., Cesar, A., Antón, R., Lopez, P., Delvalls, Á., 2009. Improved sea-urchin embryo bioassay for in situ evaluation of dredged material. Ecotoxicology 18, 1051–1057.
Pagano, G., Cipollaro, M., Corsale, G., Esposito, A., Ragucci, E., Giordano, G.G., Trieff, N.M., 1986. The sea urchin, bioassay for the assessment of damage from environmental contaminants. In: Cairns, J. Jr (Ed.), Community Toxicity Testing. American Society for Testing and Materials, Philadelphia, pp. 66–92.
Warnau, M., Iaccarino, M., De Biase, A., Temara, A., Jangoux, M., Dubois, P., Pagano, G., 1996. Spermiotoxicity and embryotoxicity of heavy metals in the Echinoid *Paracentrotus lividus*. Environ. Toxicol. Chem. 15, 1931–1936.
McClanahan, T.R., Muthiga, N.A., 2007. Ecology of Echinometra. In: Lawrence, J.M. (Ed.), Edible Sea Urchins: Biology and Ecology Developments in Aquaculture and Fisheries Science. Elsevier Science B.V, pp. 297–317.
Kominami, T., Takata, H., 2003. Timing of early developmental events in embryos of a tropical sea urchin *Echinometra mathaei*. Zool. Sci. 20, 617–626.
Mahdavi, S.N., Haghighat, K.Z., Karamzadeh, S., Naseri, F., Esteki, A.A., Rameshi, H., 2008. Reproductive cycle of the sea urchin *Echinometra mathaei* (Echinodermatidea: Echinoidea) in Bostaneh, Persian Gulf, Iran. J. Biol. Sci. 8, 1138–1148.
Sadripour, E., Mortazavi, M.S., Mahdavi Shahri, N., 2013. Effects of mercury on embryonic development and larval growth of the sea urchin *Echinometra mathaei* from the Persian Gulf. Iran. J. Fish. Sci 12, 898–907.
Boudouresque, C.F., Verlaque, M., 2007. Ecology of *Paracentrotus lividus*. In: Lawrence, J.M. (Ed.), Edible Sea Urchins: Biology and Ecology Developments in Aquaculture and Fisheries Science. Elsevier Science B.V, pp. 243–285, Edible Sea Urchins: Biology and Ecology (ed.), In J.M. Lawrence, ed..
Bellas, J., Saco-Alvarez, L., Nieto, O., Beiras, R., 2008. Ecotoxicological evaluation of polycyclic aromatic hydrocarbons using marine invertebrate embryo-larval bioassays. Mar. Pollut. Bull. 57, 493–502.
Pinsino, A., Matranga, V., Trinchella, F., Roccheri, M.C., 2010. Sea urchin embryos as an in vivo model for the assessment of manganese toxicity: developmental and stress response effects. Ecotoxicology 19, 555–562.
Gaion, A., Scuderi, A., Pellegrini, D., Sartori, D., 2013. Arsenic exposure affects embryo development of sea urchin, *Paracentrotus lividus* (Lamarck, 1816). Bull. Environ. Contam. Toxicol. 91, 565–570.
Romano, G., Costantini, M., Buttino, I., Ianora, A., Palumbo, A., 2011. Nitric oxide mediates the stress response induced by diatom aldehydes in the sea urchin *Paracentrotus lividus*. PLoS ONE 6, e25980. http://dx.doi.org/10.1371/journal.pone.0025980.
Romano, G., Russo, G.L., Buttino, I., Ianora, A., Miralto, A., 2003. A marine diatom-derived aldehyde induces apoptosis in copepod and sea urchin embryos. J. Exp. Biol. 206, 3487–3494.
Romano, G., Miralto, A., Ianora, A., 2010. Teratogenic effects of diatom metabolites on sea urchin *Paracentrotus lividus* embryos. Mar. Drugs 8, 950–967.
Chu, S.-W., Chen, S.-Y., Tsai, T.-H., Liu, T.-M., Lin, C.-Y., Tsai, H.-J., Sun, C.-K., 2003. In vivo developmental biology study using non invasive multi-harmonic generation microscopy. Opt. Express 11, 3093–3099.
Lockshin, R.A., Zakeri, Z., Tilly, J.L., 1998. When Cells Die: A Comprehensive Evaluation of Apoptosis and Programmed Cell Death. Wiley-Liss, New York.
Roccheri, M.C., Tipa, C., Bonaventura, R., Matranga, V., 2002. Physiological and induced apoptosis in sea urchin larvae undergoing metamorphosis. Int. J. Dev. Biol. 46, 801–806.
Thurber, R.V., Epel, D., 2007. Apoptosis in early development of the sea urchin strongylocentrotus purpuratus. Dev. Biol. 303, 336–346.
Agnello, M., Roccheri, M.C., 2010. Apoptosis: focus on sea urchin development. Apoptosis 15, 322–330.
Agnello, M., Filosto, S., Scudiero, R., Rinaldi, A.M., Roccheri, M.C., 2007. Cadmium induces an apoptotic response in sea urchin embryos. Cell Stress Chaperones 12, 44–50.
Rahman, M.A., Uehara, T., Aslan, L.M., 2000. Comparative viability and growth of hybrid between sympatric species of sea urchin (genus Echinometra) in Okinawa. Aquaculture 183, 45–56.
Lera, S., Pellegrini, D., 2006. Evaluation of the fertilization capability of *Paracentrotus lividus* sea urchin storage gametes by the exposure to different aqueous matrices. Environ. Monit. Assess. 119, 1–13.
Arizzi Novelli, A., Argese, E., Tagliapietra, D., Bettiol, C., Ghirardini, A. Volpi, 2002. Toxicity of tributyltin and triphenyltin towards early life stages of *Paracentrotus lividus* (Echinodermata: Echinoidea). Environ. Toxicol. Chem. 21, 859–864.
Lera, S., Pellegrini, D., 2006. Evaluation of the fertilization capability of *Paracentrotus lividus* sea urchin storaged gametes by the exposure to different aqueous matrices. Environ. Monit. Assess. 119, 1–13.
Cakal Arslan, O., Parlak, H., Oral, R., Katalay, S., 2007. The effects of nonylphenol and octylphenol on embryonic development of sea urchin (*Paracentrotus lividus*). Arch. Environ. Contam. Toxicol. 53, 214–219.
De Nicola, E., Meric, S., Gallo, M., Iaccarino, M., Della Rocca, C., Lofrano, G., Russo, T., Pagano, G., 2007. Vegetable and synthetic tannins induced hormesis/toxicity in sea urchin early development and in algal growth. Environ. Pollut. 146, 46–54.
Hsieh, C.-S., Ko, C.-Y., Chen, S.-Y., Liu, T.-M., Wu, J.-S., Hu, C.-H., Sun, C.-K., 2008. In vivo long- term continuous observation of gene expression in zebrafish embryo nerve system by using harmonic generation microscopy and morphant technology. J. Biomed. Opt. 13, 064041-1–064041-7.
Chen, I.-H., Liu, T.-M., Cheng, P.-C., Sun, C.-K., Lin, B.-L., 2001. Multimodal nonlinear spectral microscopy based on a femtosecond Cr:forsterite laser. Opt. Lett. 26, 1909–1911.
Sun, C.-K., Chu, S.-W., Chen, S.-Y., Tsai, T.-H., Liu, T.-M., Lin, C.-H., Tsai, H.-J., 2004. Higher harmonic generation microscopy for developmental biology. J. Struct. Biol. 147, 19–30.
Chu, S.-W., Chen, I.-H., Liu, T.-M., Sun, C.-K., Lee, S.-P., Lin, B.-L., Cheng, P.-C., Kuo, M.-X., Lin, D.-J., Liu, H.-L., 2002. Nonlinear bio-photonic crystal effects revealed with multimodal nonlinear microscopy. J. Microsc. 208, 190–200.
Rehberg, M., Krombach, F., Pohl, U., Dietzel, S., 2011. Label-free 3D visualization of cellular and tissue structures in intact muscle with second and third harmonic generation microscopy. PLoS One 6, e28237. http://dx.doi.org/10.1371/journal.pone.0028237.
Hsieh, C.-S., Chen, S.-U., Lee, Y.-W., Yang, Y.-S., Sun, C.-K., 2008. Higher harmonic generation microscopy of in vitro cultured mammal oocytes and embryos. Opt. Express 16, 11574–11588.

Gavrieli, Y., Sherman, Y., Ben-Sasson, S.A., 1992. Identification of programmed cell death in situ via specific labeling of nuclear DNA fragmentation. J. Cell Biol. 119, 493–501.
Fried, J., Perez, A., Clarkson, B., 1976. Flow cytofluorometric analysis of cell cycle distributions using propidium iodide. Properties of the method and mathematical analysis of the data. J. Cell. Biol. 71, 172–181.
Hamilton, M.A., Russo, R.C., Thurston, R.V., 1978. Trimmed Spearman-Karber method for estimating median lethal concentrations in toxicity bioassays. Environ. Sci. Technol. 12, 714–720.
Kobayashi, N., 1995. Bioassay data for marine pollution using echinoderms. In: Cheremisinoff, P.N. (Ed.), Environmental control technology Vol. 9. Gulf Publ., Houston, pp. 536–609.
Kobayashi, N., Okamura, H., 2004. Effects of heavy metals on sea urchin embryo development. 1 Tracing the cause by the effects. Chemosphere 55, 1403–1412.
Chaudhary, P., Gupta, A.K., 2006. Impact of water hardness and temperature on the acute toxicity of copper and mercury to a freshwater copepod, Cyclops Indian. J. Environ. Sci. 10 (2), 139–143.
Tsui, M.K., Wang, W.X., 2006. Acute, toxicity of mercury to Daphnia magna under different conditions. Environ. Sci. Technol. 40, 4025–4030.
Fernández, N., Beiras, R., 2001. Combined toxicity of dissolved mercury with copper, lead and cadmium on embryogenesis and early larval growth of the *Paracentrotus lividus* sea-urchin. Ecotoxicology 10, 263–271.
Beiras, R., Fernández, N., Bellas, J., Besada, V., González-Quijano, A., Nunes, T., 2003. Integrative assessment of marine pollution in Galician estuaries using sediment chemistry, mussel bioaccumulation, and embryo-larval toxicity bioassays. Chemosphere 52, 1209–1224.
Carballeira, C., Ramos-Gómez, J., Martín-Díaz, L., DelValls, T.A., 2012. Identification of specific malformations of sea urchin larvae for toxicity assessment: application to marine pisciculture effluents. Marine Environ. Res. 77, 12–22.
Ianora, A., Miralto, A., Poulet, S.A., Carotenuto, Y., Buttino, I., Romano, G., Casotti, R., Pohnert, G., Wichard, T., Colucci-D'Amato, L., et al., 2004. Aldehyde suppression of copepod recruitment in blooms of a ubiquitous planktonic diatom. Nature 429, 403–407.
Buttino, I., Pellegrini, D., Romano, G., Hwang, J.-S., Liu, T.-M., Sartori, D., Sun, C.-K., Macchia, S., Ianora, A., 2011. Study of apoptosis induction in Acartia tonsa nauplii exposed to chronic concentration of Nickel. Chem. Ecol. 27, 97–104.
Buttino, I., Hwang, J.-S., Sun, C.-K., Hsieh, C.-T., Liu, T.-M., Pellegrini, D., Ianora, A., Sartori, D., Romano, G., Cheng, S.-H., Miralto, A., 2011. Apoptosis to predict copepod mortality: state of the art and future perspectives. Hydrobiologia 666, 257–264.
Voronina, E., Wessel, G.M., 2001. Apoptosis in sea urchin oocytes, eggs, and early embryos. Mol. Reprod. Dev. 60, 553–561.
Filosto, S., Roccheri, M.C., Bonaventura, R., Matranga, V., 2008. Environmentally relevant cadmium concentrations affect development and induce apoptosis of *Paracentrotus lividus* larvae cultured in vitro. Cell Biol. Toxicol. 24, 603–610.
Sutton, D.J., Tchounwou, P.B., 2006. Mercury-induced externalization of phosphatidylserine and caspase 3 activation in human liver carcinoma ($HepG_2$), cells. Int. J. Environ. Res. Public Health 3, 38–42.
Hsieh, C.-S., Ko, C.-Y., Chen, S.-Y., Liu, T.-M., Wu, J.-S., Hu, C.-H., Sun, C.-K., 2008. In vivo long- term continuous observation of gene expression in zebrafish embryo nerve system by using harmonic generation microscopy and morphant technology. J. Biomed. Opt. 13, 064041-1–064041-7.
Bonacker, D., Stiber, T., Wang, M., Bhöm, K.J., Prots, I., Unger, E., Their, R., Bolt, H.M., Degen, G.H., 2004. Genotoxicity of inorganic mercury salts based o disturbed microtubule function. Arch. Toxicol. 78, 575–583.
Bischof, J.C., Padanilam, J., Holmes, W.H., Ezzell, R.M., Lee, R.C., Tompkins, R.G., Yarmush, M.L., Toner, M., 1995. Dynamics of cell membrane permeability changes at supraphysiological temperatures. Biophys. J. 68, 2608–2614.
Parran, D.K., Mundy, W.R., Barone, Jr. S., 2001. Effects of methylmercury and mercuric chloride on differentiation and cell viability in PC12 cells. Toxicol. Sci. 59, 278–290.
Hajela, R.K., Peng, S.Q., 2003. Comparative effects of methylmercury and Hg^{2+} on human neuronal N and R type high voltage activated calcium channels transiently expressed in human embryonic kidney 293 cells. J. Pharmacol. Exp. Therap. 306, 1129–1136.
Allemand, D., De Renzis, G., Payan, P., Girard, J.-P., Vaissiere, R., 1988. $HgCl_2$-induced cell injury. Differential effects on membrane-located transport systems in unfertilized and fertilized sea urchin eggs. Toxicology 50, 217–230.
Allemand, D., De Renzis, G., Payan, P., 1993. Effects of $HgCl_2$ on intracellular pH in sea urchin eggs : activation of H^+ excretion and Na^+/H^+ exchange activity. Aquat. Toxicol. 26, 171–184.
Viarengo, A., 1989. Heavy metals in marine invertebrates: mechanisms of regulation and toxicity at the cellular level. CRC Crit. Rev. Aquat. Sci. 1, 295–317.
Rieger, A.M., Hall, B.E., Luong, I.E.T., Schang, L.M., Barrreda, D.R., 2010. Conventional apoptosis assays using propidium iodide generate a significant number of false positives that prevent accurate assessment of cell death. J. Immunol. Methods 358, 81–92.